JOURNAL OF COMPUTATIONAL PHYSICS 66, 324–331 (1986)

Accessibility of Second Regions of Stability in Tokamaks

J. MANICKAM

*Plasma Physics Laboratory, Princeton University,
Princeton, New Jersey 08544*

Received August 13, 1985

DEDICATED TO THE MEMORY OF RAYMOND C. GRIMM

Second regions of stability to the ideal ballooning modes have been shown to exist in large-aspect-ratio circular and small-aspect-ratio bean-shaped tokamaks. We report on the existence of these second stability regions in finite-aspect-ratio D-shaped tokamaks. We also report on the discovery of a second-stable region with respect to the $n = 1$ external kink mode in a bean-shaped plasma. The role of the shear and current profile in determining these regions of parameter space are discussed. © 1986 Academic Press, Inc.

INTRODUCTION

Stability to ideal MHD modes is an important element of tokamak design and operation. It is well known that tokamaks display second regions of stability to ballooning modes [1 − 5]. This refers to the situation where, as the plasma pressure $\beta \equiv 2\mu_0\langle p\rangle/\langle B^2\rangle$ is increased, there is a threshold for the onset of ballooning modes. Further increasing the pressure opens the possibility of a self-healing process, where the plasma sufficiently strengthens its local shear to stabilize the ballooning modes and enters a second region of stability. These results were initially obtained in large-aspect-ratio tokamaks and attempts to induce them in small-aspect-ratio systems were unsuccessful. Then, the effects of shaping the plasma cross section were explored, leading to the discovery of a second region of stability in plasmas with a bean-shaped cross section. In fact, it was discovered that with careful shaping of the cross section and current profile, it is possible to eliminate the region of instability, giving direct and continuous access to the second-stable region [6]. In this report, we present a study of a D-shaped tokamak, where we have also obtained direct access to the second-stable region.

Kink modes represent a more dangerous instability in tokamak operation. They tend to have lower thresholds for onset and are often considered to set the beta limit in present devices [7]. They are, however, amenable to stabilization by placing a conducting shell close to the plasma surface. Here we report on the possibility of stabilizing them in a bean-shaped plasma by shaping the current profile. We dis-

0021-9991/86 $3.00

cuss the role of the magnetic shear and current profile in determining the stability properties and present results for a D-shaped tokamak stable to ballooning modes and a bean-shaped one stable to both kink and ballooning modes at high beta.

Role of Magnetic Shear and Current Profile

It is well known that magnetic shear plays an important role in determining the stability properties of a plasma. Thus, when considering ballooning modes, it is observed [6, 8] that the local shear

$$S \equiv -\frac{\mathbf{B}\times\nabla\Psi}{|\nabla\Psi|^2}\cdot\nabla\times\frac{\mathbf{B}\times\nabla\Psi}{|\nabla\Psi|^2}$$

is a key equilibrium characteristic that helps to determine stability. Further, when the global shear $dq/d\Psi$ is small, it is possible to reverse the sign of S and enhance stability. On the other hand, it is well known that increasing $dq/d\Psi$ promotes stability to the external kink mode. Another important equilibrium parameter is the pressure gradient $dp/d\Psi$, which appears in combination with the curvature κ_Ψ. While the shear terms are stabilizing, the pressure gradient and curvature term are destabilizing for ballooning modes.

The authors in Ref. [6] exploited the possibility of enhancing the outward magnetic shift, which has the effect of strengthening the poloidal magnetic field by indenting the plasma on the small-major-radius side. This was shown to shift the contour of vanishing S away from the region of unfavorable curvature, leading to stability to ballooning modes. Here we recognize that the quantity $\kappa_\Psi dp/d\Psi$ can also be exploited to improve the stability. The weak spot in the magnetic field is located where $S=0$, the quantity $\kappa_\Psi dp/d\Psi$, represents the driving force. Hence, we can avoid instability if we can reduce or eliminate $\kappa_\psi dp/d\psi$ wherever $S=0$. This can be achieved by choosing pressure profiles which are flattened to make $dp/d\Psi$ small in regions where $S=0$ lies in the unfavorable curvature side.

It is well known that the driving force for the external kink mode is the current gradient dj/dr [9, 10]. In conventional tokamaks this is expected to remain negative as the current decreases from the magnetic axis towards the plasma edge. However, it is possible to reverse the current-density gradient while retaining a monotonically increasing q-profile. This is accomplished by choosing a broad pressure profile which has a larger gradient near the outside. Then, increasing β while holding q fixed, as in a flux-current tokamak (FCT) sequence, results in a current-density profile that increases radially outward. When this reversal is strong enough, we expect the kink mode to be stabilized.

Numerical Techniques

In this study, we have obtained equilibria for stability analysis using a flux coordinate code [11] with a specified shape for the outermost plasma surface. This shape is defined by,

$$x(\theta) = R - b + (a + b\cos\theta)\sin(\theta + \delta\sin\theta),$$

$$z(\theta) = Ea\sin(\theta),$$

where $0 < \theta < 2\pi$, R represents the major radius, a the minor radius, E the ellipticity, δ the triangularity, and b the indentation. The current profile is specified through $q(\Psi)$ and $p(\Psi)$ as

$$q(\Psi) = q_0 + q_1\Psi^{\alpha_1} + q_2\Psi^{\alpha_2},$$

$$p(\Psi) = p_0[(1 - \Psi^{\beta_1}) + p_2\Psi^{\beta_2}(1 - \Psi)^{\beta_3}],$$

where Ψ varies from 0on axis to unity at the plasma edge, and q_0, q_1, q_2, α_1, α_2, β_1, β_2, β_3 are constants for a sequence of FCT equilibria with p_0 varying to provide different β values.

The equilibria are analyzed for stability to the $n = 1$ external kink and ballooning modes using the scalar δW stability code, Pest–2 [12], and the ballooning analysis code [13]. To ensure accuracy of the equilibrium we use a mesh with 56 radial points and 160 poloidal points. Selected equilibria are obtained with 80 radial points to verify convergence of the results. The stability analysis is done with 201 radial and 128 poloidal grid points, with 31 fourier harmonics to resolve the poloidal mode structure.

Results

D-Shaped Plasma

We investigate the stability of a family of D-shaped equilibria, Fig. 1(a). These

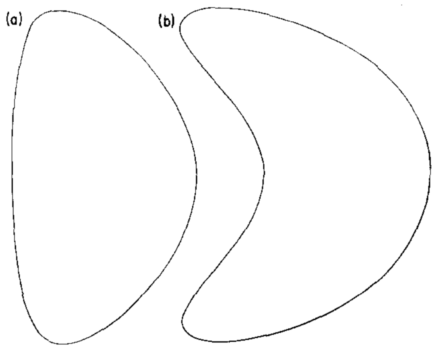

FIG. 1. (a) D-shaped tokamak plasma cross section with $R = 1$, $a = 0.25$, $E = 1.8$, $\delta = 0.5$, $b = 0.0$; (b) bean-shaped plasma cross section with $R = 1$, $a = 0.2$, $E = 2$, $\delta = -0.5$, $b = 0.4$. This plasma cross-section has an indentation of 0.33.

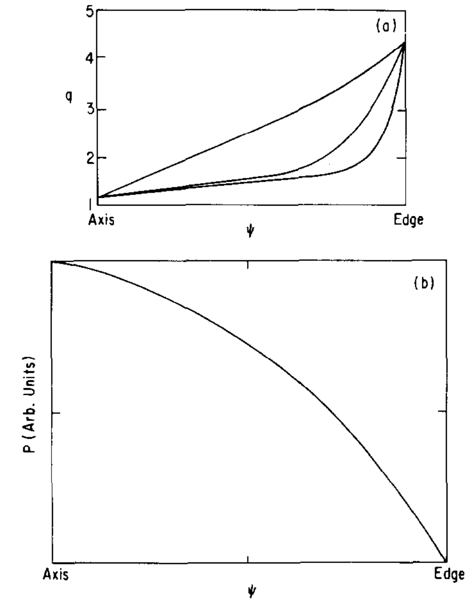

FIG. 2. (a) Representative q profiles used in Fig. 3; $q_0 = 1.05$, $q_1 = 3.05$, $\alpha_1 = 1.1$, 3 and 6, and $q_2 = 0$. (b) The pressure profile given by $\beta_1 = 1.6$, $\beta_2 = 3$, $\beta_3 = 1.2$, and $p_2 = 1$.

equilibria are characterized by having the same boundary shape, pressure profile form, q axis, and q edge. The detailed shape of the q profile is varied by changing α_1; see Fig. 2. The profiles shown correspond to three selected values of α_1 which effectively determines the average global shear. Figure 3 summarizes the stability properties of this family of equilibria. Note that a vertical line on this plane would correspond to a sequence of FCT equilibria. The solid curves shown connect the critical betas for the kink and ballooning modes for the different shear sequences.

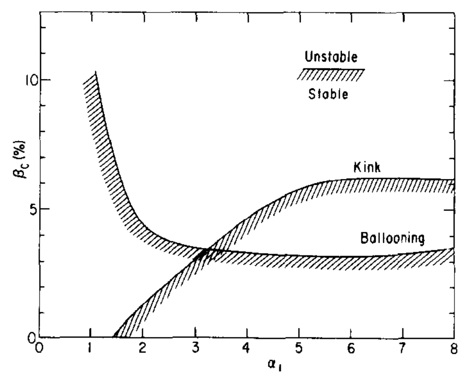

FIG. 3. β_{crit} for the $n = 1$ external kink and ballooning modes as a function of the shear parameter α_1 for the dee-shaped plasma cross-section of Fig. 1a.

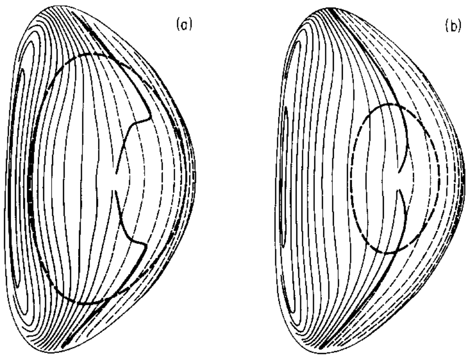

FIG. 4. Contours of $\kappa_\psi p'$, with solid contours indicating favorable regions with positive curvature and broken contours unfavorable regions with negative curvature. The heavy solid line connects the points of vanishing local shear S. The heavy broken line shows the most unstable surface with respect to ballooning modes. (a) $\alpha_1 = 3$ and (b) $\alpha_1 = 1.1$.

We observe a systematic dependence on the global shear. In particular, the kink-mode limit is highest at large values of the global shear, while the ballooning-mode limit is highest at small average global shear. These results are readily interpreted in the light of our earlier discussion on the role of magnetic shear. Figure 4 provides a graphic demonstration of the role of the local shear. Here we note, Fig. 4a, that the surface with the maximum growth rate for ballooning modes passes through the point where $\kappa_\psi p'$ has a maximum unfavorable value on the line of vanishing local shear. Reducing the global shear, Fig. 4b, shifts the $S = 0$ line so that we need a larger value of p' to destabilize the ballooning mode. Modifying the pressure profile by flattening it in this region would further enhance the stability. Figure 5 shows a second profile with reduced p' near the axis. This, in fact, results in complete stabilization of the ballooning modes and represents a breakthrough to the region of second stability in the same sense as achieving direct access to the second region of stability at large indentation, as shown in Ref. [6]. We have carefully examined the FCT sequence from this profile and have found complete stability to ballooning modes up to β-values of 27%. Equilibrium constraints prevent us from seeking a region of instability at even higher β. These equilibria are quite unstable to the external kink mode, but are stabilized with a wall at a distance of 0.2 plasma radii from the plasma boundary.

Figure 3 also shows the $n = 1$ external kink mode stability for the original sequence. At large global shear, we find that the kink limit rises well above the balloon limit. This improved stability to kink modes is attributable, in part, to the strengthening of the local shear, but more importantly, it is due to the strong deformation of the current profile with increased β, Fig. 6. In particular, we note that this choice of pressure profile tends to concentrate the current density near the edge of the plasma and, as β increases, the average value of dj/dr decreases and the β limit rises. Here we note that while the kink limit is high, the balloon limit is low.

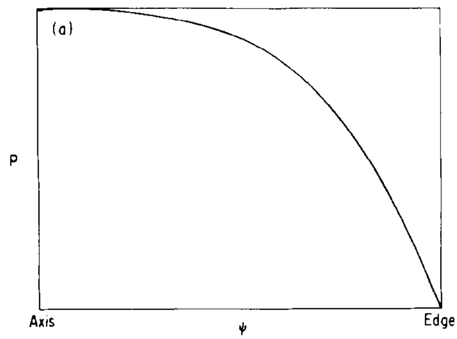

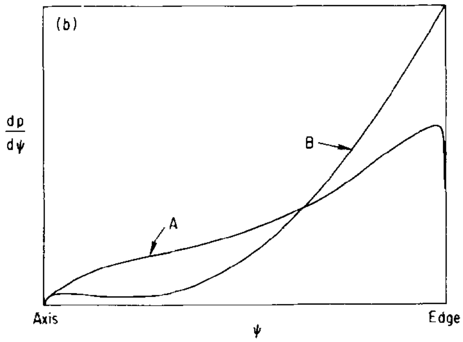

FIG. 5. (a) Modified pressure profile that permits access to the second region of stability. $\beta_1 = 1.5$, $\beta_2 = 2$, $\beta_3 = 1$, and $p_2 = 2$. (b) Comparison of p' for the profiles of Figs. 2b, curve A, and 5a, curve B.

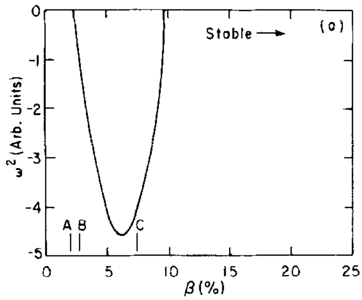

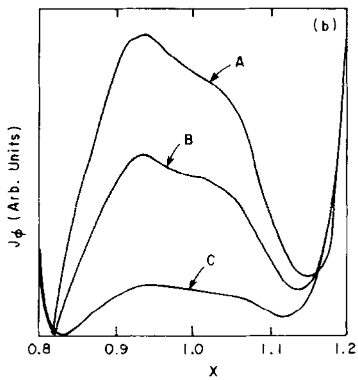

FIG. 6. (a) Growth rate for $n = 1$ external kink mode versus β for the bean-shaped plasma of Fig. 1b, with the pressure profile of Fig. 5. (b) The cross section of the toroidal current density at $z = 0$ for the indicated values of β. Note that the scales are different.

We remedy this by using a bean-shaped cross section which has improved stability to ballooning modes and seek stability to both modes simultaneously.

Bean-Shaped Plasma

We investigate the stability of a strongly indented bean-shaped plasma, Fig. 1b, with a current profile chosen to have large global shear, $q_0 = 1.1$, $q_1 = 1.5$, $q_2 = 2.5$, $\alpha_1 = 2$, and $\alpha_2 = 10$. We use the same pressure profile that led to the second region of stability for ballooning modes in the D-shaped plasmas. We find that as β is increased instability to the $n = 1$ external kink modes sets in, and as β is further increased the growth rate peaks and then drops back to zero as the second region of stability to the kink mode is reached, Fig. 6. We have examined this sequence up to $\beta \approx 20\%$ without encountering another region of instability. We note from Fig. 6b, that as β is increased, the current profile peaks more strongly on the outside until the average dj/dr reverses its sign. We believe that this reversal is responsible for stabilizing the kink mode. These equilibria have also been examined for stability to ballooning modes and are stable up to the highest β studied.

Discussion

In this report we have examined the role of magnetic shear in determining the stability of the external $n = 1$ kink and ballooning modes and have emphasized the value of tailoring the current profile to achieve stability to these modes. In particular, we note that reducing the average global shear and tailoring p' to be small in the region of bad curvature where the local shear vanishes permits access to the second region of stability in a Dee-shaped plasma. In the case of the kink mode, we demonstrate that tailoring the current profile so that dj/dr on average reverses its sign leads to a second region of stability. In practice we realize that generating and sustaining such current profiles in an experiment would be difficult, if not impossible. However, the value of this study lies in opening new avenues of approach to high-β regions by emphasizing the role of the current profile. Further studies to understand the properties of these regions, as well as their accessibility in a more realistic manner are in progress.

Acknowledgments

I wish to acknowledge many useful discussions with several members of the Princeton Plasma Physics Laboratory Research Staff: Drs. A. H. Boozer, M. S. Chance, J. L. Johnson, D. A. Monticello, and P. H. Rutherford. In particular I am grateful to Dr. J. L. Johnson and Dr. J. Hastie, a visiting scientist from the UKAEA, for many useful and inspirational discussions. Finally, I acknowledge the unstinting help of Mr. Arthur Miller in the extensive computer studies required for this report.

I dedicate this paper to the memory of Dr. Raymond C. Grimm, a dear friend and colleague, who was largely responsible for introducing me to this field of research.

This work was supported by United States Department of Energy Contract DE-AC02-76-CHO-3073.

REFERENCES

1. B. COPPI, A. FERREIRA, AND J. J. RAMOS, *Phys. Rev. Lett* **44**, 990 (1980).
2. D. LORTZ AND J. NÜHRENBERG, *Phys. Rev. Lett. A* **68**, 49 (1978).
3. H. R. STRAUSS, W. PARK, D. A. MONTICELLO, R. B. WHITE, S. C. JARDIN, M. S. CHANCE, A. M. M. TODD, AND A. H. GLASSER, *Nucl. Fusion* **20**, 638 (1980).
4. C. MERCIER, in *Plasma Physics and Controlled Nuclear Fusion Research* (International Atomic Energy Agency, Vienna, 1979), Vol. I, 701.
5. L. SUGIYAMA AND J. W. K. MARK, *Phys. Lett. A* **84**, 123 (1981).
6. M. S. CHANCE, S. C. JARDIN, AND T. H. STIX, *Phys. Rev. Lett.* **51**, 1963 (1983).
7. F. TROYON, R. GRUBER, H. SAURENMANN, S. SEMENZATO, AND S. SUCCI *Plasma Phys. and Contr. Fusion* **26**, 209 (1984).
8. J. M. GREENE AND M. S. CHANCE, *Nucl. Fusion* **21**, 453 (1981).
9. J. WESSON, *Nucl. Fusion* **18**, 87 (1978).
10. V. D. SHAFRANOV, *Zh. Tech. Fiz.* **40**, 241 (1970); *Sov. Phys.-Tech. Phys.* **15**, 175 (1970).
11. J. DELUCIA, S. C. JARDIN, AND A. M. M. TODD, *J. Comput. Phys.* **37**, 183 (1980).
12. R. C. GRIMM, R. L. DEWAR, AND J. MANICKAM, *J. Comput. Phys.* **49**, 94 (1983).
13. D. DOBROTT, D. B. NELSON, J. M. GREENE, A. H. GLASSER, M. S. CHANCE, AND E. A. FRIEMAN, *Phys. Rev. Lett.* **39**, 943 (1977).